Arch. Metall. Mater. **66** (2021), 4, 1087-1094

DOI: 10.24425/amm.2021.136428

S. PRAVEEN KUMAR[1], S. M. SENTHIL[1*], R. PARAMESHWARAN[1], R. RATHANASAMY[1]

FABRICATION OF A NOVEL SILVER-BASED ELECTRICAL CONTACT COMPOSITES AND ASSESSMENT OF ITS MECHANICAL AND ELECTRICAL PROPERTIES

The electrical contactors play a crucial role in closing the circuit in many power distribution components like overhead lines, underground cables, circuit breakers, transformers, and control systems. The failure in these components mainly occurs due to the break-down of contactors due to the continuous opening and closing action of contacts. Silver (Ag)-based oxide contact materials are widely used in practice, among which silver tin oxide ($AgSnO_2$) is most common. An attempt is made in increasing the performance of $AgSnO_2$, by adding Tungsten Oxide (WO_3) in various weight proportions, thus finding the optimal proportion of $AgSnO_2WO_3$ to have increased mechanical and electrical performances. All the composite samples are fabricated in-house using powder metallurgy process. The assessment of physical and electrical properties namely, density, hardness, porosity, and electrical conductivity, showed that 90%Ag-8.5%SnO_2-1.5%WO_3 composite yielded superior results. With help of morphological tests, wear characteristics are also investigated, which showed that 90%Ag-8.5%SnO_2-1.5%WO_3 composite has a wear coefficient of 0.000227 and a coefficient of friction of 0.174 at an optimized load of 10 N and sliding velocity of 0.5 mm/s.

Keywords: silver tin oxide, electrical contact, composites, tungsten oxide, conductivity

1. Introduction

The use of electrical switching appliances and machinery is widely increasing in modern days. Contactors play a critical role of closing the circuit, holding the current at the contact points without any electro-thermo-mechanical interference, interrupting the circuit at times of need, and extending the loop for full number of operations without degradation using contact points with ideal property [1,2] shown in Table 1.

For sake of higher electrical conductivity, precious metals such as silver (Ag), gold (Au) or platinum (Pt) and base metals such as copper (Cu) and aluminum (Al) contact materials are used over the past two decades. However, the property of high electrical conductivity alone doesn't meet the requirements for the contact materials [3]. The evaluation of Metal Matrix Composite (MMC) based on AgMeO resulted in improved mechanical properties with a nominal reduction in electrical conductivity compared to other precious materials [4,5]. AgCdO is a best

TABLE 1

Properties required for a contact material

S. No.	Properties	Required level	Reason
1.	Electrical conductivity	High	Limits the heat generation during the conduction of current
2.	Thermal conductivity	High	Dissipates arc heat and resistance developed
3.	Reaction resistance to environment	High	Avoids the formation of insulation oxides, sulfides, and other compounds
4.	Melting point	High	Limits arc erosion, transfer of metals and welding and sticking phenomenon of contacts
5.	Hardness	Good	Provides wear resistance
6.	Ductility	Good	Ease of fabrication
7.	Density	Average	Higher thermal conductivity
8.	Material and processing cost	Low	Reduces the overall cost of the appliances
9.	Porosity	Low	Effective flow of electrons

[1] KONGU ENGINEERING COLLEGE, ERODE, TAMILNADU, INDIA

* Corresponding author: senthil.awaits@gmail.com

suited electrical contact material as it meets all the required properties like good electrical conductivity, hardness, wear resistance and anti-welding properties that a contact point should possess [6-8]. The toxic nature of cadmium oxide (CdO) has an environmental concern, and it is necessary to choose environmentally sustainable alternative materials [9,10]. Scientists are researching various environmentally friendly products according to the stringent environmental regulations as per Restriction of Hazardous Substances (RoHS) and Waste Electrical and Electronic Equipment (WEEE) Directive [11,12].

Silver tin oxide ($AgSnO_2$) and silver-zinc oxide (AgZnO) have emerged as promising alternatives as a substitute for AgCdO [5,15] and silver graphite (AgC) [13,14]. Yet, $AgSnO_2$ contact materials have poor conduct at high temperatures, poor workability and high contact resistance due to the coalescence of SnO_2 on the Ag matrix surface [16]. To overcome, ternary MeOs like Copper Oxide (CuO), Indium Oxide (In_2O_3), Tungsten Oxide (WO_3) or Bismuth Oxide (Bi_2O_3) are added as additives to $AgSnO_2$ base [12,16-18]. Even a 0.5 wt.% of WO_3 addition with the $AgSnO_2$ base using Powder Metallurgy (PM) technique strengthens the $AgSnO_2$ base's tribological and morphological behaviours [16,17]. Yet, the property enhancement by varying the weight % of WO_3 is still impending [16,18]. An attempt has been made for improving the properties of the $AgSnO_2WO_3$ contact materials by varying the weight percentage of WO_3 by compensating SnO_2. Addition of WO_3 aids in decreasing the duration of arc formation and changes of arc erosion along with transfer of materials while making and breaking a circuit [33]. For varied input parameters at different levels, it becomes essential to identify the process parameters for obtaining the optimized results [18]. For identifying the optimized process parameters, ANOVA can be used [34].

2. Materials and methods

2.1. Fabrication of Ag-SnO_2-WO_3 contact materials

In the present study, the metal base powders of Ag, SnO_2, and WO_3 with a recommended grain size of 1-2 microns are purchased from Alfa Aesar Inc., UK [12,19,20]. Weight percentage of metal base powder samples for processing by PM technique is shown in Table 2. The usual PM processing of Ag based electrical contact materials initially involves dry homogenization of powder mixtures by manual mixing [16,21]. The blend is then compacted at 100 MPa using a hydraulic press, followed by sintering in an electro-resistive oven at 850°C for 2 hours [32]. It is then die-forged at 80 MPa for 30 minutes at around 750 to 820°C, subsequently annealing at 750°C, and finally quenching in water [16,22]. The sintered components are then formed into tablets of size Ø5 mm × 14.5 mm by the forging process as shown in Fig. 1.

2.2. Assessment of physical, tribological and morphological properties

Physical properties like density, hardness, electrical conductivity, and porosity are measured as per ASTM standards for

TABLE 2

Comparison of the physical and electrical properties of $AgSnO_2WO_3$ contact materials

Sample No.	Weight Percentage (%)			Density (g/cc)	Hardness (HV5)	Porosity (%)	Electrical conductivity (% IACS)
	Ag	SnO_2	WO_3				
1	90	10	0	8.92	58.23	3.65	44.82
2	90	9.5	0.5	8.46	62.8	2.54	44.43
3	90	9	1	8.53	64	2.51	44.20
4	90	8.5	1.5	8.44	65.72	2.53	44.80
5	90	8	2	8.52	63.27	3.05	26.92
6	90	7.5	2.5	7.48	63.55	3.56	15.34

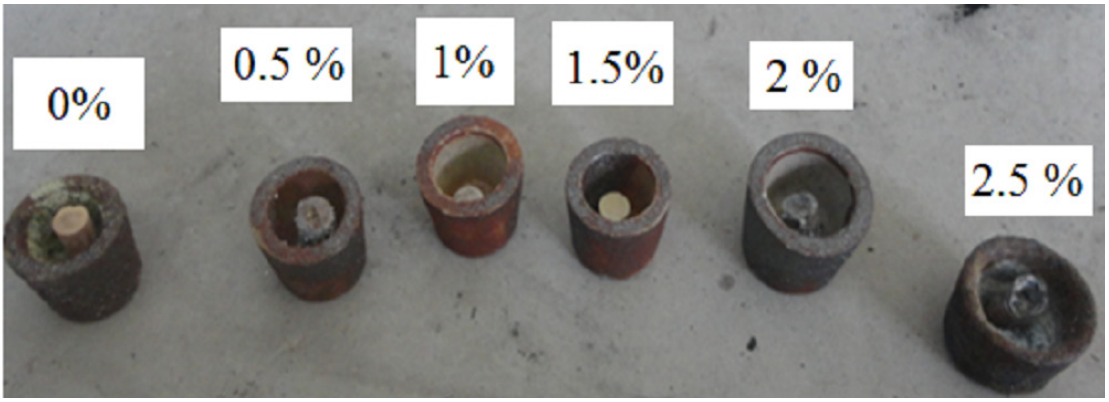

Fig. 1. Sintered $AgSnO_2WO_3$ tablets kept in a graphite crucible

contact materials and the properties are compared as discussed in [31]. A traditional pin-on-disc tribometer with a pin pressed against a rotating disc is considered in this study. The pin is kept overhanging over a stiff lever designated as frictionless force transducer. Based on the normal force produced by the dead weight, the frictional force is evaluated from the deflection of the elastic arm and measurement is done using inductive displacement transducers. The wear properties are measured as per the ASTM G99 standard using a Pin-On-Disc (POD) equipment with wear track measuring of about 50 mm and constant sliding distance of 10,000 m [10,23]. The pin weight is measured before and after the wear test to identify the loss in mass using Eq. (1) and Eq. (2).

$$\text{Wear coefficient, } (\text{WC}) = \frac{Loss\ in\ mass}{Load\ x\ sliding\ distance} \quad (1)$$

$$\text{Coefficient of friction, } (\text{COF})\ (\mu) = \frac{Friction\ force}{Normal\ load} \quad (2)$$

While contacting, the contact points of an electromechanical contactor do not involve the influence of lubricant fluids. Hence, dry sliding wear condition is considered. Based on the Maxwell's pulling force , electromagnetic force exerted by the movable contact over stationary contacts is selected as 2 N, 5 N, and 10 N [24]. The sliding velocity is varied between 0.3-1 m/s [25]. For this wear study, the sliding velocities considered are 0.5 m/s, 1 m/s, and 2 m/s. The rotating disc of POD is made up of steel EN 31 with wear track of 50 mm. ANOVA are performed for determining the optimal sliding velocity and normal load for the contactor application. A full factorial experimental design is selected to assess the WC and COF, using Minitab 17.

3. Results and discussion

3.1. Assessment of the physical properties of $AgSnO_2WO_3$ contact materials

The fabricated materials are subject to testing for physical properties and the average values are presented in Table 2. Further, a comparison plot depicting the variations in the physical properties of $AgSnO_2WO_3$ contact materials is shown in Fig. 2. With the addition of WO_3 into the $AgSnO_2$ base, the density of the materials varies from 8 g/cm^3 to 9 g/cm^3, for the addition of up to 2 weight percentage (samples 2-5). The density of the material gets decreased to 7.48 g/cm^3 by the addition of 2.5 weight percentage of WO_3 (sample 6). This 2.5 weight percentage of WO_3 in turn increases the porosity value of the contact material. This may be due to inadequate coalescence between the materials and oxides formed over the surface [10]. From the comparison plot, it is evident that as the weight percentage of WO_3 increases,

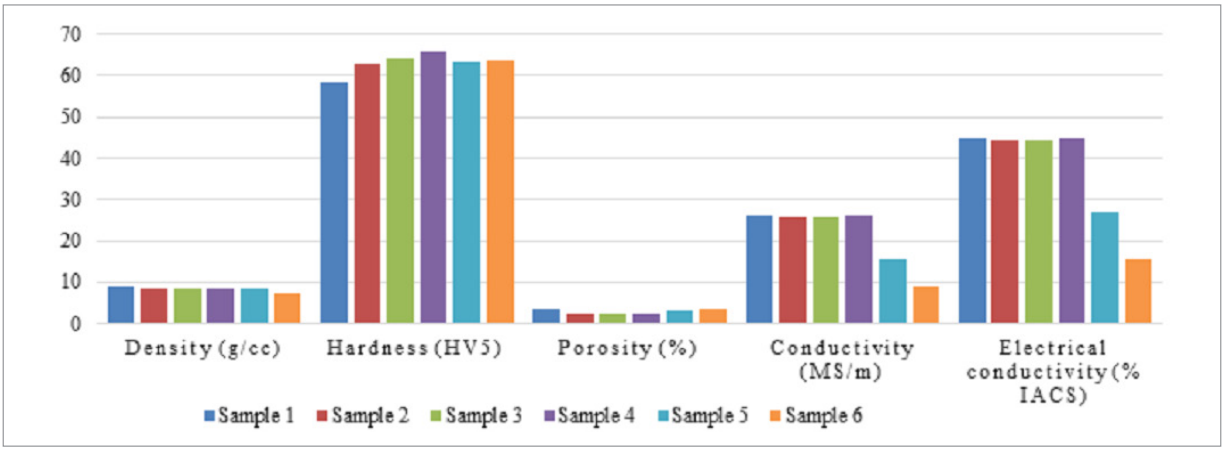

Fig. 2. Comparison of the physical and electrical properties of $AgSnO_2WO_3$ contact materials

TABLE 3

DOE for determining WC and COF

DOE			Before wear		After wear		Parameters	
Exp. No.	Load (N)	Sliding Velocity (m/s)	Initial Mass (g)	Density (g/cc)	Final Mass (g)	Mass Loss (g)	WC	COF (μ)
1	2	0.5	9.938	8.44	9.921	0.0167	0.000198	0.212
2	2	1	9.254	8.42	9.237	0.0166	0.000197	0.2
3	2	2	9.342	8.50	9.326	0.0162	0.00019	0.198
4	5	0.5	9.926	8.43	9.891	0.0347	0.000206	0.197
5	5	1	9.891	8.40	9.857	0.0343	0.000204	0.184
6	5	2	9.188	8.36	9.156	0.0334	0.0002	0.182
7	10	0.5	9.221	8.39	9.125	0.0956	0.000228	0.175
8	10	1	9.254	8.42	9.161	0.0926	0.00022	0.166
9	10	2	9.949	8.45	9.857	0.0917	0.000217	0.164

the hardness value of $AgSnO_2WO_3$ increases (samples 1-4) and reaches the maximum value of 67.72 HV5 with 1.5% of addition (sample 4). Further addition of WO_3 leads to a decrease in hardness value around 63 HV5 as identified in samples 5 & 6. Up to the addition of 2 weight percentage of WO_3 (sample 2-5), the porosity value is maintained around 3%. This proves that the addition of the minimum percentage of WO_3, ranging from 0.5% to 2% has improved the wetting behaviour of the material. In the same way, a decreasing trend is observed in the electrical conductivity with the increase in the weight percentage of WO_3 (Sample nos.: 1-4). The level of decrease in electrical conductivity is the bare minimum that the meagre addition of WO_3 does not show any significant change in the plot. The addition of 2% and 2.5% of WO_3 (Sample 5 & 6) has drastically reduced the electrical conductivity of the contact material fabricated. This may be due to the deposition of tungsten over the surface [26] as it has lesser electrical conductivity than the Ag matrix. The residual stresses induced within the sample would have created an increase in electrical resistivity and thereby reducing the conductivity of the sample material.

From the physical property plots and the comparison of the relative weights in Table 4, it's confirmed that the addition of 1.5% WO_3 proves to provide the highest hardness, higher electrical conductivity, lowest porosity, and relatively low density which are relevant for electrical contact applications. Thus, the sample 4 ($AgSnO_2$-1.5WO_3), having a respective combination of 90-8.5-1.5, is taken for further study of morphological and tribological characteristics and compared with sample 1, which is pure $AgSnO_2$.

3.2. Morphological studies of fabricated $AgSnO_2$ and $AgSnO_2$-1.5WO_3 contact materials

3.2.1. SEM analysis of surface texture of fabricated $AgSnO_2$ and $AgSnO_2$-1.5WO_3 contact materials

SEM micrograph of $AgSnO_2$ and $AgSnO_2$-1.5WO_3 contact materials are shown in Fig. 3(a) and 3(b) respectively. In Fig. 3(a), an even dispersion of reinforced particles is identi-

TABLE 4

ANOVA for WC and COF of $AgSnO_2$-1.5WO_3

ANOVA for WC					
Source	DF	Adj SS	Adj MS	F-Value	P-Value
Load	2	0.000052	0.000026	48.85	0.005
Sliding Velocity	2	0.000120	0.000060	111.51	0.002
Error	4	0.000002	0.000001		
Total	8	0.002160			
Model Summary					
S	R-sq	R-sq (adj)	R-sq (pred)		
0.0007328	99.93%	99.80%	98.93%		
ANOVA for COF					
Source	DF	Adj SS	Adj MS	F-Value	P-Value
Load	2	0.001844	0.000922	9.19	0.043
Sliding Velocity	2	0.000310	0.000155	13.54	0.031
Error	4	0.000006	0.000001		
Total	8	0.002160			
Model Summary					
S	R-sq	R-sq (adj)	R-sq (pred)		
0.0000012	99.63%	99.00%	96.54%		

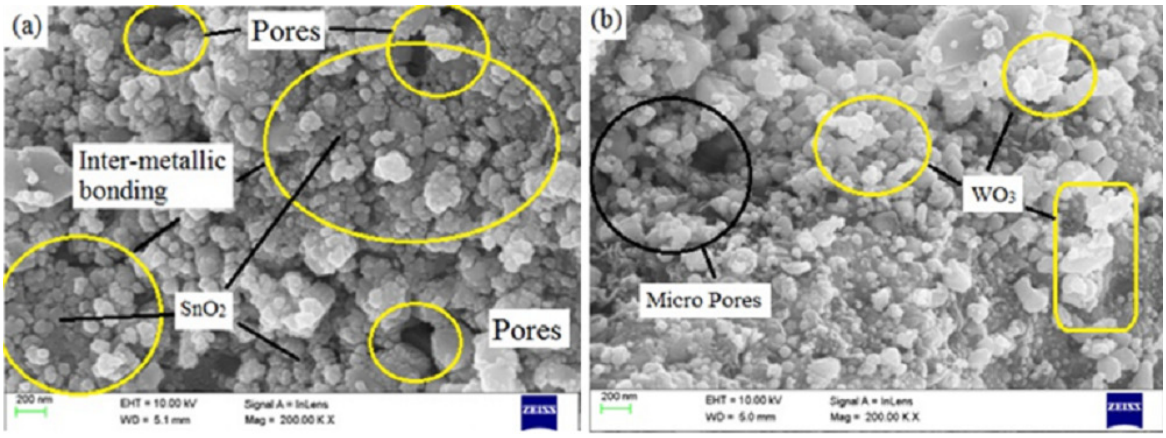

Fig. 3. Surface texture of (a) $AgSnO_2$ and (b) $AgSnO_2$-1.5WO_3

fied over the polished surface of the fabricated $AgSnO_2$contact material. Pores and formation of craters are observed over the surface of the fabricated $AgSnO_2$ contact material in a large number. The reinforced materials get dispersed in the base matrix with a higher porosity percentage. Fig. 3(b) shows the SEM micrograph of $AgSnO_2$-1.5WO_3. Agglomerates of WO_3 are detected all over the surface, as the same phenomenon for WO_3 addressed in literature [27]. Ag matrix gets solidified beneath, leaving the traces of WO_3 particles over the surface. The 1.5 weight percentage addition of WO_3 has increased the coalescence of SnO_2 with the base Ag matrix, thus yielding the properties of contact material in an enhanced manner [28].

3.2.2. XRD Analysis of fabricated $AgSnO_2$ and $AgSnO_2$-1.5WO_3 contact materials

From the XRD reports shown in Fig. 4 and 5, the presence of SnO_2 and WO_3 dispersed over the Ag matrix is determined. The presence of inter-metallic components, namely $AgSnO_2$ and Ag_2O are identified at the peaks between 30-40°2θ and between 60-70°2θ respectively (Fig. 4). From Fig. 5, the presence of tungsten oxide and tin oxide is identified at the peaks between 40-50°2θ and 70-80°2θ respectively when compared with library data [29]. The XRD pattern indicates a single-phase with monoclinic structure, and the peak intensities and positions are comparable with the base JCPDS Card No. 32-1395 for WO_3 and Card No. 88-0287 for SnO_2 (°2θ for SnO_2 = 26.9, 34.3, 38.9, 52.1, 62.1 and 65.8). Intermetallic component formation aids in improving the microhardness value of the component. Again, the variation of Ag_2O within the limits 1 wt% and 3 wt % may improve the microhardness value [33].

3.3. Tribological studies of $AgSnO_2$-1.5WO_3 pin

Surface wear morphology is determined for the compositions with $AgSnO_2$-1.5WO_3 using the POD equipment. 9 samples with 90%Ag-8.5%SnO_2-1.5%WO_3 are prepared using the PM technique. The responses for WC and COF are computed ex-

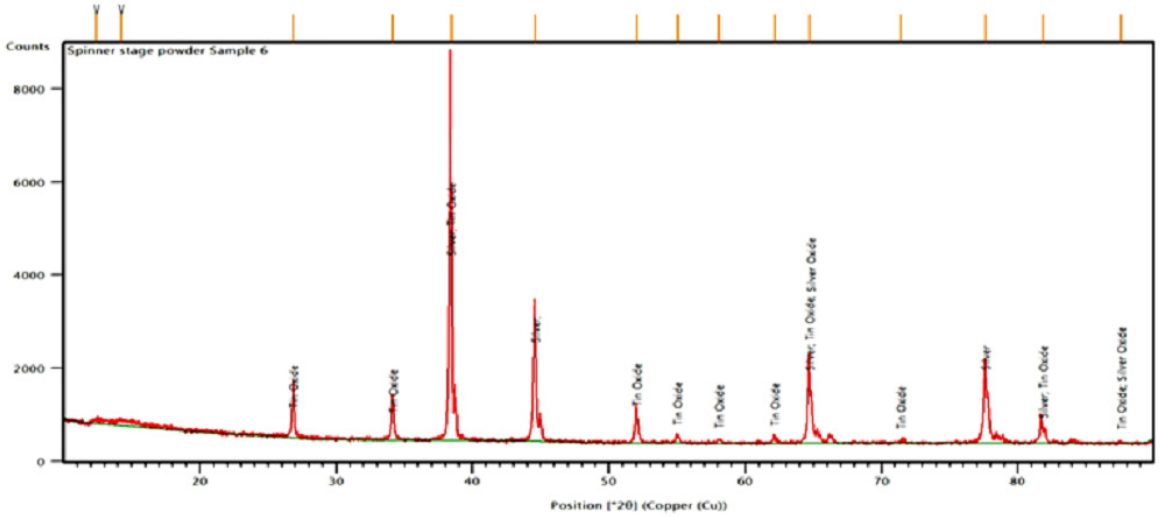

Fig. 4. XRD plot on contact material $AgSnO_2$

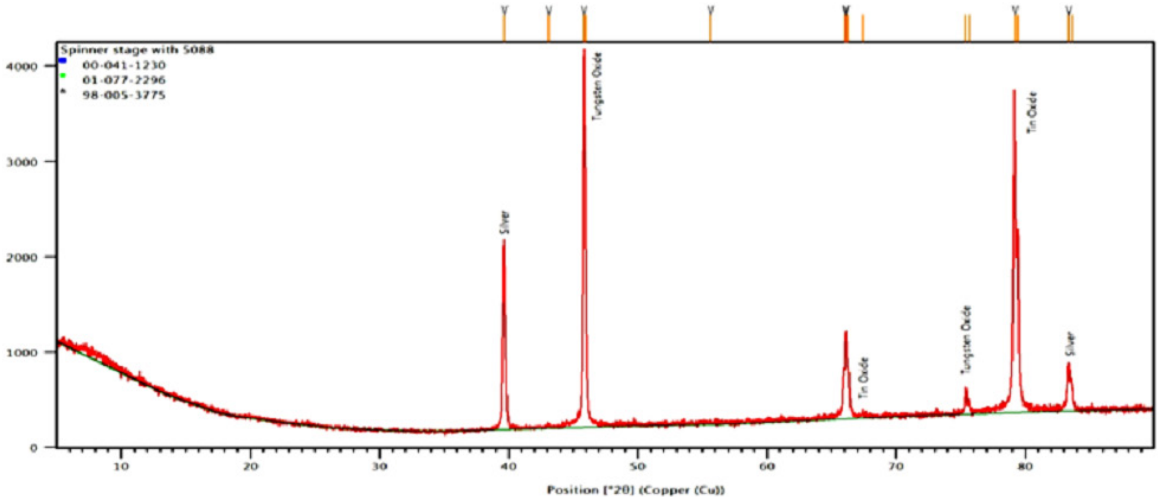

Fig. 5. XRD plot on contact material $AgSnO_2$-1.5WO_3

perimentally using POD equipment and the results are presented in Table 3. Analysis of Variance (ANOVA) for WC and COF is given in Table 4. The adjusted R square value obtained for WC and COF is 97.31% and 99.47% respectively, which implies the reliability of the data acquired from the experimentation procedure. Based on the ANOVA table, sensitivity of predicted value is up-to 96.54 %. Fig. 6(a) and Fig. 6(b) shows the residual plots of WC and COF respectively for $AgSnO_2$-1.5WO_3 material. The normal probability plots for both WC and COF show the residual values fitted along a straight line with minimum variations proving that the errors have a normal distribution. Comparing the residual values and the fitted values for both WC and COF, the fit values are scattered throughout the area without forming any pattern as in run order plot. This validates the experimentation process and the determination of both WC and COF. Fig. 7(a) shows the main effects plot for the signal-to-noise ratio considering WC to be the minimum value. Even at a normal load of 10 N and sliding velocity of 0.5 m/s, the material with $AgSnO_2$-1.5WO_3 shows minimal WC. The main effects plot shown in Fig. 6(b) provides a better COF when applying a load of 2 N and maintaining a sliding velocity of 0.5 m/s.

3.3.1. SEM analysis of surface wear morphology of worn-out $AgSnO_2$-1.5WO_3contact point

Table 5 provides the results for WC and COF of $AgSnO_2$-1.5WO_3 material at 10 N load and 0.5 m/s velocity. Fig. 8 shows the SEM micrograph of the surface texture of the worn-out surface of the $AgSnO_2$-1.5WO_3 contact material obtained from the confirmation test. Fig. 8(a) reveals the wear surface morphology showing a strong ploughing and adhesion kind of

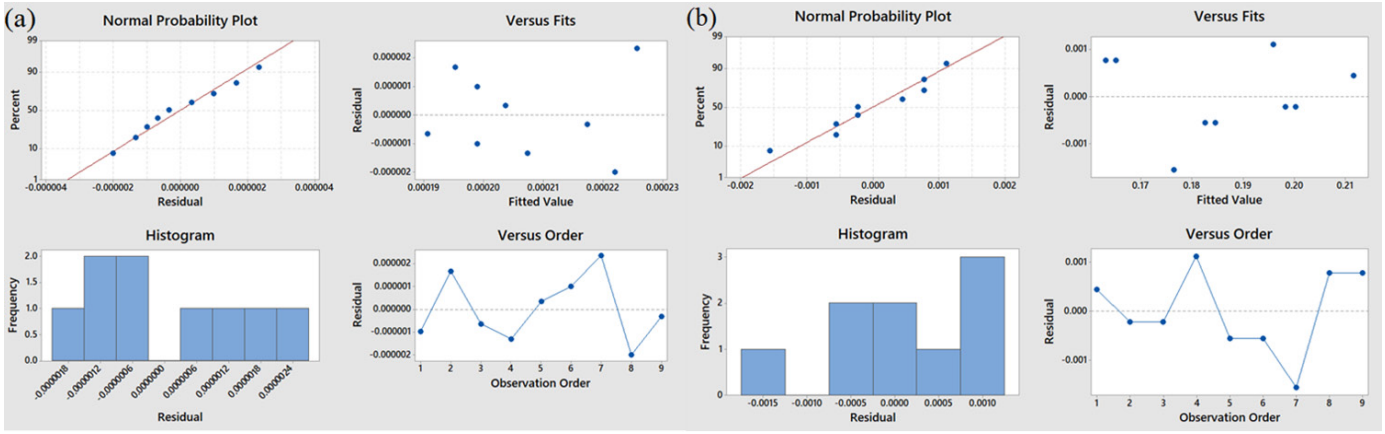

Fig. 6. Residual plots for (a) WC & (b) COF of $AgSnO_2$-1.5WO_3

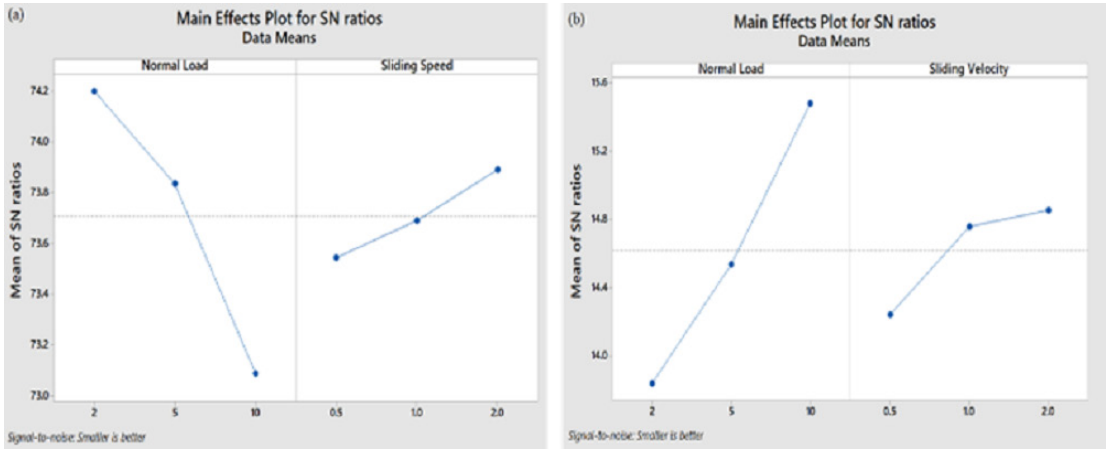

Fig. 7. Main effects plot for signal-to-noise ratio for (a) WC and (b) COF of $AgSnO_2$-1.5WO_3

TABLE 5

Confirmation result for $AgSnO_2$-1.5WO_3 pin with optimized parameters

DOE		Before wear		After wear		Parameters	
Load (N)	Sliding Velocity (m/s)	Initial Mass (g)	Density (g/cc)	Final Mass (g)	Mass Loss (g)	WC	COF (μ)
10	0.5	9.221	8.39	9.125	0.0956	0.000227	0.174

wear phenomenon over the surface of the contact material. The aggregates of wear particles are found over the surface of the contact material (pin). Portions of flake off region, breaking of the grain, ranges of plastic deformation, structure, and crushing of fragments are observed in Fig. 8(a). Similar surface morphology on the friction surface is found in the literature [30]. Weak inter-metallic zones are evident along with alternate deep and shallow grooves at various portions as seen in Fig. 8(b). Aggregates of wear particles are also seen as the frictional motion continues in the same location and direction.

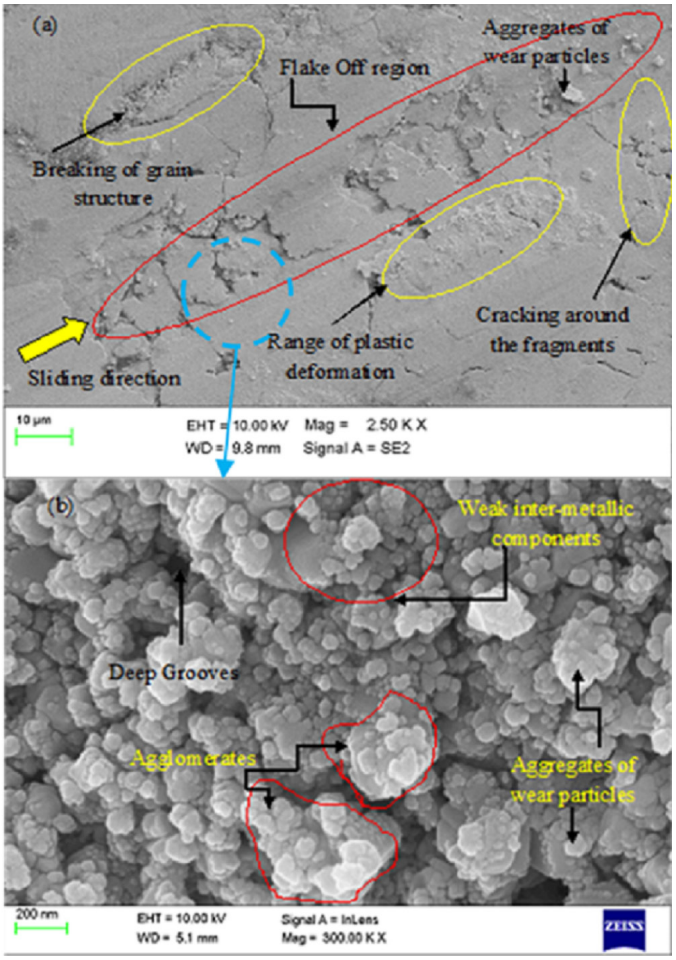

Fig. 8. SEM micrograph of the wear surface morphology of $AgSnO_2$-$1.5WO_3$ at (a) low magnification and (b) high magnification

4. Conclusion

Thus, an attempt in introducing a new material for electrical contactors is made. Keeping the weight percentage of Ag as constant at 90 %, $AgSnO_2WO_3$ contact material is fabricated by varying the weight percentage of WO_3 is as 0, 0.5, 1, 1.5, 2, and 2.5 by compensating the equivalent weight percentage in SnO_2. The physical and electrical properties are measured and compared between the samples, based on which $AgSnO_2$-$1.5WO_3$ is found to have better properties. Also, morphological and tribological studies are carried out to measure the performance of the fabricated $AgSnO_2$-$1.5WO_3$. The tribological behavior of $AgSnO_2$-$1.5WO_3$ contact material is assessed by calculating WC and COF using POD equipment based on the full factorial design involving two factors at three levels. Based on the results obtained from the above research, the following conclusions are made:

- The hardness of base $AgSnO_2$ has increased from 58.23 HV to 65.72 HV upon addition of 1.5% WO_3 and reduced the values of density and porosity from 8.92 g/cm^3 and 3.65% respectively to 8.44 g/cm^{3}and 2.53% respectively.
- The electrical conductivity is retained almost similar during 1.5 weight percentage addition of WO_3 when comparing the base $AgSnO_2$.
- The assessment of the physical properties of $AgSnO_2WO_3$ with 90-8.5-1.5 respective weight percentages proves to deliver higher hardness, high electrical conductivity, acceptable density, and low porosity values. Whereas the addition of more than 2 weight percentage of WO_3, these properties see an empirical deterioration.
- For the 90%Ag8.5%$SnO_2$1.5%WO_3 material, WC and COF values are assessed to be 0.000227 and 0.174 respectively under an optimal normal load of 10 N, and the corresponding sliding velocity is identified as 0.5 m/s.
- Formations of new phases was not identified instead some portions of flake off region, breaking of the grain, ranges of plastic deformation, structure, and crushing of fragments are observed over the surface of the pin post wear.
- Reducing the weight percentage of Ag by 10% economically aids in the reduction of 12.52% of the cost incurred for Ag for a single contact point and around 22% of cost reduction can be achieved for a single contact pair. This provides an economic contactor without compromising the properties of the contact material.

Additionally, wear surface morphology analyzed using SEM micrograph reveals adhesion type of surface wear behaviour for the 90%Ag8.5%$SnO_2$1.5%WO_3 contact material. This study can be further extended by measuring the fatigue life of the material which is yet another essential property for electrical contactors.

Acknowledgement

The authors would like to thank Kongu Engineering College for extending laboratory facilities towards successful completion of this research work.

Funding

This research did not receive any specific grant from funding agencies in the public, commercial, or not-for-profit sectors.

Conflicts of interest/Competing interests

The authors declare that they have no conflict of interest

REFERENCES

[1] P.B. Joshi, N.S.S. Murti, V.L. Gadgeel, V.K. Kaushik, J. Mater. Sci. Lett. **14** (16), 1099-1101 (1995). DOI: https://doi.org/10.1007/BF00423372

[2] P.B. Joshi, P. Ramakrishnan, Materials for electrical and electronic contacts: processing, properties, and applications, Science Pub Inc. (2004).

[3] Z. Ying, W. Jingqin, K. Huiling, IEEE T. Comp. Pack. Man. **9** (5), 864-870 (2018). DOI: https://doi.org/10.1109/TCPMT.2018.2882237

[4] P.B. Joshi, V.J. Rao, B.R. Rehani, A. Pratap, Silver-Zinc oxide electrical contact materials by mechanochemical synthesis route (2007).

[5] B. Holm, Northwest coast Indian art: An analysis of form. University of Washington Press (2017).

[6] O. Nilsson, F. Hauner, D. Jeannot, Replacement of AgCdO by AgSnO/sub 2/in DC contactors, In Proceedings of the 50th IEEE Holm Conference on Electrical Contacts and the 22nd International Conference on Electrical Contacts Electrical Contacts. (pp. 70-74). IEEE (2004 September). DOI: https://doi.org/10.1109/HOLM.2004.1353097

[7] D.A. Romanov, S.V. Moskovskii, E.A. Martusevich, E.A. Gayevoy, V.E. Gromov, Structural-phase state of the system "CdO-Ag coating/copper substrate" formed by electroexplosive method. Metalurgija **57** (4), 299-302 (2018).

[8] P.G. Slade, R.K. Smith, Electrical switching life of vacuum circuit breaker interrupters. In Electrical Contacts-2006. Proceedings of the 52nd IEEE Holm Conference on Electrical Contacts (pp. 32-37). IEEE (2006, September). DOI: https://doi.org/10.1109/HOLM.2006.284061

[9] S.H. Choi, B. Ali, S.Y. Kim, S.K. Hyun, S.J. Seo, K.T. Park, J.S. Park, Int. J. Appl. Ceram. Tec. **13** (2), 258-264 (2016). DOI: https://doi.org/10.1111/ijac.12478

[10] C. Wu, Q. Zhao, N. Li, H. Wang, D. Yi, W. Weng, J. Alloy Compd. **766**, 161-177 (2018). DOI: https://doi.org/10.1016/j.jallcom.2018.06.317

[11] J.L. Wintz, S. Hardy, Design guideline of contactors: optimal use of assembled contacts. In 2013 IEEE 59th Holm Conference on Electrical Contacts (Holm 2013) (pp. 1-10). IEEE (2013, September). DOI: https://doi.org/10.1109/HOLM.2013.6651406

[12] N.M. Talijan, V. Ćosović, J. Stajić-Trošić, A. Grujić, D. Živkovic, E. Romhanji, J. Min. Metall. B. **43** (2), 171-176 (2007). DOI: https://doi.org/10.2298/JMMB0702171T

[13] B. Rehani, P.B. Joshi, P.K. Khanna, J. Mater. Eng. Perform. **19** (1), 64-69 (2010). DOI: https://doi.org/10.1007/s11665-009-9437-3

[14] P.G. Slade, (Ed.), Electrical contacts: principles and applications, CRC press (2017).

[15] M.W. Richert, J. Richert, A. Hotloś, P. Pałka, W. Pachla, M. Perek-Nowak, In Mater. Sci. Forum. **667**, 145-150 (2011). DOI: https://doi.org/10.4028/www.scientific.net/MSF.667-669.145

[16] V. Ćosović, N. Talijan, D. Živković, D. Minić, Z. Živković, J. Min. Metall. B. **48** (1), 131-141 (2012).

[17] K. Wojtasik, W. Missol, Metal Powder Report **59** (7), 34-39 (2004). DOI: https://doi.org/10.1016/S0026-0657(04)00206-1

[18] M. Lungu, S. Gavriliu, T. Canta, M. Lucaci, E. Enescu, J. Optoelectron. Adv. M. **8** (2), 576 (2006).

[19] V. Ćosović, M.M. Pavlović, A. Cosovic, P. Vulić, M. Premović, D. Živković, N.M.Talijan, Sci. Sinter. **45** (2), 173-180 (2013). DOI: https://doi.org/10.2298/SOS1302173C

[20] N.M. Talijan, Zaštitamaterijala **52** (3), 173-180 (2011).

[21] M. Mustapha, F. Mustapha, O. Mamat, P. Hussain, Powder Metall. **54** (3), 343-353 (2011). DOI: https://doi.org/10.1179/003258909X12573447241581

[22] N.M. Talijan, V.R. Ćosović, A.R. Ćosović, D.T. Živković, Metallurgical and Materials Engineering **18** (4), 259-272 (2012).

[23] M. Braunovic. IEICE T. Electron. **92** (8), 982-991 (2009). DOI: https://doi.org/10.1587/transele.E92.C.982

[24] A. Dogariu, S. Sukhov, J. Sáenz, Nat. Photonics. **7** (1), 24-27 (2013). DOI: https://doi.org/10.1038/nphoton.2012.315

[25] M. Taher, F. Mao, P. Berastegui, A.M. Andersson, U. Jansson, Tribol. Int. **119**, 680-687 (2018). DOI: https://doi.org/10.1016/j.triboint.2017.11.026

[26] F. Findik, H. Uzun, Mater. Design **24** (7), 489-492 (2003). DOI: https://doi.org/10.1016/S0261-3069(03)00125-0

[27] B.A. Wasmi, A.A. Al-Amiery, A.A.H. Kadhum, A.B. Mohamad, J. Nanomater. (2014).

[28] M. Lungu, S. Gavriliu, D. Patroi, M. Lucaci, Adv. Mat. Res. **23**, 103-106 (2007). DOI: https://doi.org/10.4028/www.scientific.net/AMR.23.103

[29] M. Raja, J. Chandrasekaran, M. Balaji, P. Kathirvel, Optik **145**, 169-180 (2017). DOI: https://doi.org/10.1016/j.ijleo.2017.07.049

[30] E. Harea, I. Lapsker, A. Laikhtman, L. Rapoport, L. Tribol, Lett. **52** (2), 205-212 (2013).

[31] S. Praveen Kumar, R. Parameshwaran, A. Ananthi, J. JenilJaba Sam, Arch. Metall. Mater. **62** (2017). DOI: https://doi.org/10.1515/amm-2017-0287

[32] S.P. Kumar, R. Parameshwaran, S.A Kumar, S. Nathiya, K. Heenalisha, Mater. Today-Proc. (2020). DOI: https://doi.org/10.1016/j.matpr.2020.05.666

[33] H. Li, X. Wang, Y. Xi, Y. Liu, X. Guo, Mater. Design. **121**, 85-91 (2017). DOI: https://doi.org/10.1016/j.matdes.2017.02.059

[34] Mohd Shahadan Mohd Suan, Nurulhawa Ali Hasim, Mohd Edeerozey Abd Manaf, Mohd Rafie Johan, Chinese J. Phys. **55** (5), 1857-1864 (2017). DOI: https://doi.org/10.1016/j.cjph.2017.08.012